Realization and MIMO-link Measurements of a Transmit Module for Spatial Modulation

Jo Verhaevert[1], Patrick Van Torre[1]

[1]Industrial Technology & Construction, Ghent University, Valentin Vaerwyckweg 1, B-9000 Gent,

Jo.Verhaevert@UGent.Be, Patrick.VanTorre@UGent.Be

***Abstract*—This paper describes the realization of a circuit that transmits a data stream, through spatial modulation in the 2.45 GHz frequency band. The development of the transmitter includes RF circuit design with components such as a PLL synthesizer, Tx-DAC and IQ-modulator. A microcontroller, integrated into the circuit and programmed in C, is at the heart of the system.**

In this hardware system, developed specifically for spatial modulation, data is BPSK modulated and transmitted through an RF switch connected to two antennas. It can differ for every symbol which antenna is used, according to an extra series of information bits that are to be transmitted. Here the number of the selected antenna encodes the extra information bit per symbol, which not only results in a doubling of the data rate but also realizes diversity. Spatial modulation allows these features with only a single hardware transmit chain, resulting in low-cost and low-complexity hardware. At the receiving side, the extra information bits are decoded by assessing the channel used for each symbol.

This practical system has been thoroughly tested by means of different measuring campaigns. The measurement results show that spatial modulation is correctly demodulated at the receiving side and forms an effective way to realize affordable MIMO systems.

***Index Terms*—RF-design, MIMO, modulation, spatial modulation.**

I. Introduction

As more and more wireless applications arise, with more and more users who each demand a higher data rate, the continuous development of more and more advanced wireless technology is required. On top of that, the radio spectrum and available bandwidth is limited. Transmitting more and more data within the same bandwidth by increasing the spectral efficiency forms a great challenge.

Different techniques exist to obtain a higher data rate within the same bandwidth. MIMO (Multiple Input, Multiple Output) systems effectively increase the data rate, but require full hardware transmit or receive chains connected to each antenna, resulting in complex and expensive systems.

One of the latest techniques to economically increase spectral efficiency, is spatial modulation, where a MIMO system can be realized with only one transmit chain [1]. A stream of additional information bits, synchronous to the modulated symbols, selects a transmit antenna number as a function of these information bits. Based on its channel estimation information, the receiver is able the decide which antenna transmitted each particular symbol, effectively recovering the stream of extra information bits. This transmission scheme offers significant advantages in comparison to a SISO (Single Input, Single Output) system, at a very limited extra cost.

In this paper, the design and practical implementation of a transmitter for spatial modulation is described with two transmit antennas. Using BPSK (Binary Phase Shift Keying) modulation and switching between antenna 1 or 2 based on the extra information bits to be transmitted, the data rate and spectral efficiency are doubled effectively. Section II handles the hardware design for the transmit circuit, whereas Section III focuses on the control software and the processing at the receiver. Section IV documents the measurement results, illustrating that the transmit design is realized successfully. Finally, the conclusions are listed in section V.

II. Transmitter

Figure 2 contains the block diagram of the transmitter. The central part is the Silicon Laboratories C8051F320 microcontroller [2], which is clocked by an external 24 MHz crystal oscillator. In the final lay-out the microcontroller is placed at the backside of the PCB, to limit the interference to the RF components, which are all on the opposite side of the board's ground plane.

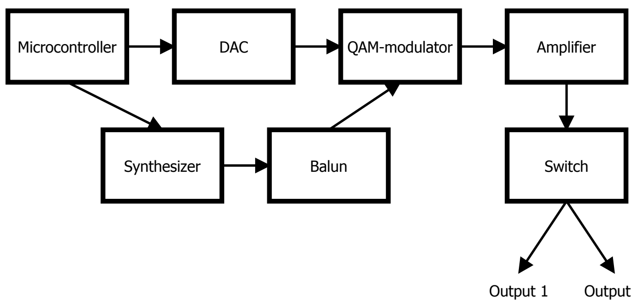

Fig. 2. The block diagram of the transmitter.

The DAC (Digital to Analog Convertor) of the block diagram is an AD9761 [3], providing analog baseband signals to the modulator. In order to modulate the data, an AD8346 IQ-modulator [4] is used, allowing QAM- or phase-modulation.

The Mini-Circuits DSN-2520A-219A+ RF frequency synthesizer [5], a hybrid component including a PLL and VCO, is employed to accurately generate the carrier frequency within the 2.45 GHz frequency band. The external reference crystal

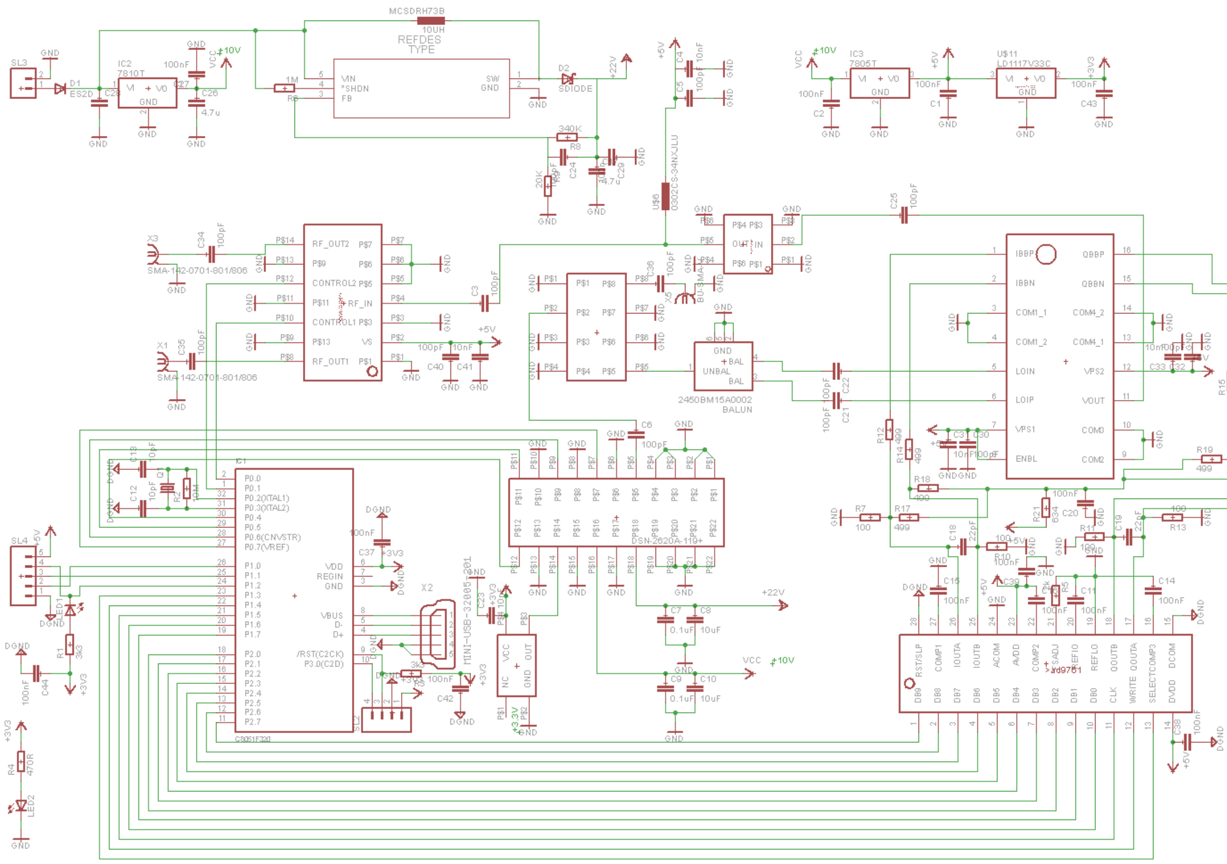

Fig. 1. Full circuit diagram of the 2-antenna spatial modulation transmitter.

oscillator FOX-HC736R-20 [6] operates at a frequency of 20 MHz, with ±25 ppm stability. The balun in the block diagram transforms the synthesized carrier into a differential signal, as required for the balanced operation of the IQ-modulator's internal circuitry. The final power amplifier HXG-242+ has an amplification of 13.6 dB, specified at 2.36 GHz [7]. Driven by the extra information bits, the RSW-2-25P+ [8] switches the RF-signal between both transmit antennas, providing the Spatial Modulation. The latter switching operation is performed during the zero-crossings of the transmitted pulses, in order to prevent abrupt transitions and hence limit the transmission bandwidth.

The design of the PCB is realized using Cadsoft Eagle [9], for the circuit diagram and board design. The diagram of the complete circuit is displayed in Figure 1. In the bottom left corner of it, the microcontroller as heart of the circuit can be seen. The microcontroller is connected with its neighbour the frequency synthesizer, which is also controlled by it. At the bottom right, the DAC can be seen, which is connected via the IQ-modulator above at the right and the balun to the left of it, to the RF-switch. This switch is also controlled via the microcontroller and is connected to the antennas via SMA-connectors.

The PCB implementation is shown in Figure 3. Although all RF paths are kept as short as possible, inevitably some signal radiation of the PCB occurs, given the small wavelength of 12 cm at 2.45 GHz. To shield the PCB, an aluminum enclosure is used, with only the grounded SMA antenna connectors at the outside (at the right on Figure 3). Please note that the power supply enters the casing by means of a feed-through capacitor, allowing only the DC voltage and not the RF-signals to cross the shielding.

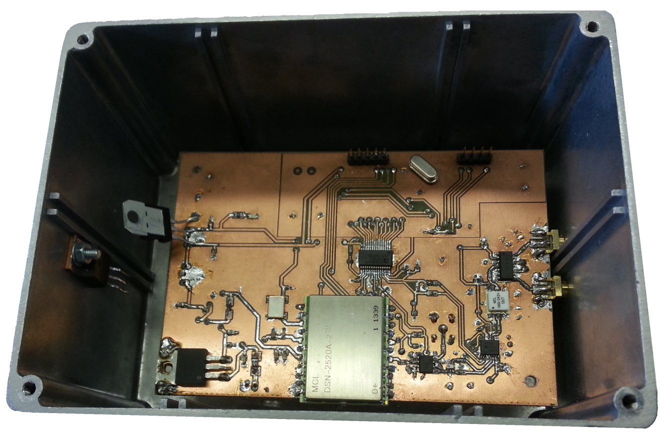

Fig. 3. The realized PCB with complete circuit of the transmitter.

III. SOFTWARE AND PROCESSING

The microcontroller controls the complete system and generates I- and Q-signals via the DAC. In order to detect the difference between both antennas in the received signals, pilot symbols are used. Those are a fixed sequence of pseudo random symbols, which is known at the receiver side. Because the transmit antennas are separated in space, the transmitted signals have phase and amplitude differences at the receiver side. Based on channel estimation the receiver can estimate from which antenna exactly each symbol has been transmitted.

The receiving part of the MIMO communication system is a Signalion HaLo430 [10] which transfers the sampled received signals, at 4 different receiving antennas, to Matlab for postprocessing. The receiving antennas are the elements of a Tip-Truncated Equilateral Microstrip Patch Antenna (ETMPA) array [11], [12]. The antenna elements are positioned at a center-to-center distance of 92 mm, corresponding to $3/4\lambda$ at 2.45 GHz.

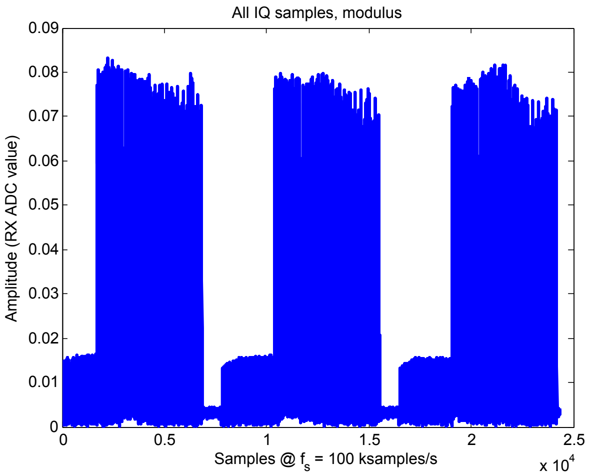

Fig. 4. Pilots and data.

The received Matlab data provides I- and Q-samples. After removing the DC-offset, the signal is downsampled by a factor 100, resulting in a sample rate of 100 ksamples/sec. In Figure 4 the frames, consisting of 2 pilot sequences followed by the data symbol sequence, are displayed. Clearly, the signals from one antenna experience more fading than those from the other antenna, resulting in a detectable difference in amplitude between both received signals. Note that the detection of the selected antenna uses the amplitude as well as the phase of the received symbols and estimated channels, implicating that even equal-gain channels can be distinguished, based on their phase difference.

In processing the received signal, coarse time synchronization is performed, searching for the sequence of pilot symbols, the data and the gap between them. The Oerder & Meyr algorithm [13], further provides fine time synchronization, indicating the optimal sample moments for the symbols (corresponding to the center of the opening in an eye-diagram).

IV. MEASUREMENT RESULTS

In this section, measurement results are shown, with the PCB shielded by the aluminum case. A Non Line-of-Sight (NLoS) configuration was selected, with the anechoic chamber in between transmitter and receiver and approximately 8 m separation. The propagation path hence can be via reflection against the wall, resulting in a specular component and a Quasi NLOS configuration. There is an orientation difference of 90° between both whip antennas and for both antennas an angle of approximately 45° with respect to the ground. Also note that no coaxial cables are used and the whip antennas are connected directly to the SMA-connectors of the aluminum case.

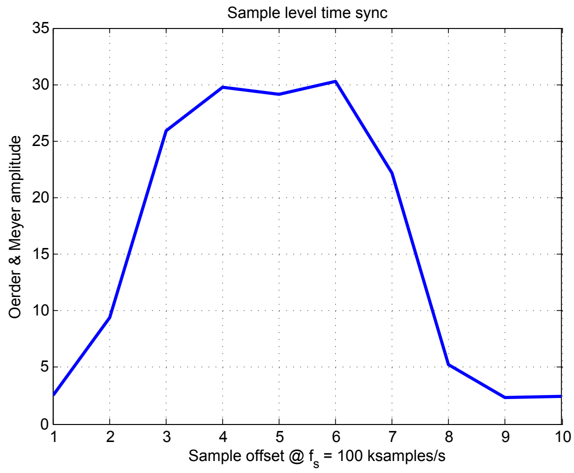

Fig. 5. Oerder and Meyr time synchronization.

The Oerder & Meyr algorithm described earlier results in Figure 5, where a maximum occurs at the best sampling time, being every sixth sample in this case. The signal is now decimated by keeping only every sixth sample.

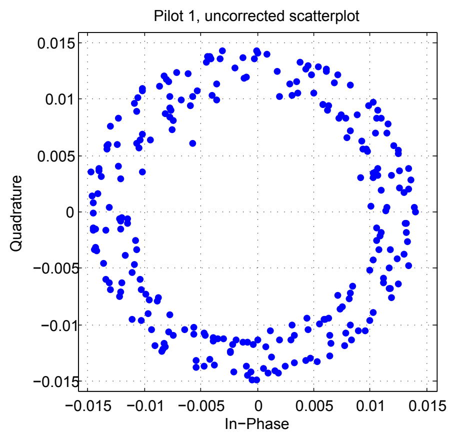

Fig. 6. Uncorrected scatterplot for pilot 1.

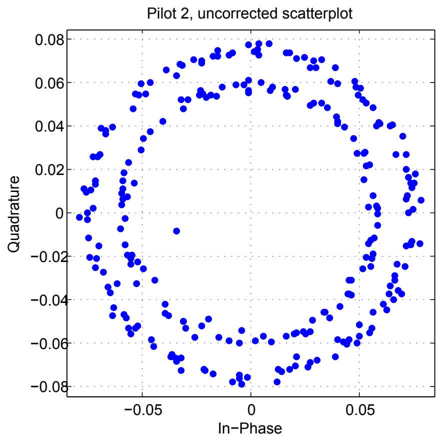

Fig. 7. Uncorrected scatterplot for pilot 2.

Even a small frequency offset between the oscillators at the transmitter and receiver results in a rotation of the received constellation over $360°$, and hence needs to be compensated for. The error on the crystal frequency at the transmitter side is specified at 25 ppm, whereas an error of 1 ppm on a frequency of 2.45 GHz already results in a frequency error of 2450 Hz. The uncorrected scatter plot in the IQ-plane is given in Figure 6 for pilot 1 and for pilot 2 in Figure 7. Please note the weaker received amplitude level of pilot 1 in comparison to pilot 2.

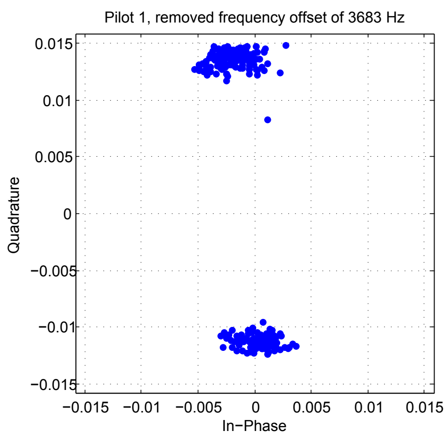

Fig. 8. Scatterplot with compensated frequency offset for pilot 1.

The next step in the processing is now estimating this frequency offset and compensating for it, in order to eliminate the constellation rotation. The software iteratively compensates the received signal for frequency offsets within a given range and selects the result with the least residual rotation in the IQ-plane. In the particular case documented here, a frequency offset of 3683 Hz is removed and the results are depicted in Figure 8. The frequency offset of the second pilot sequence is also compensated for with the same offset and the resulting constellation is shown in Figure 9.

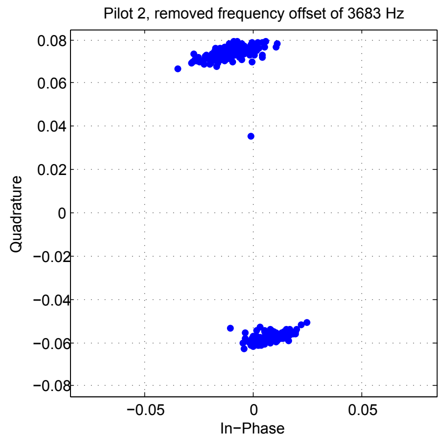

Fig. 9. Scatterplot with compensated frequency offset for pilot 2.

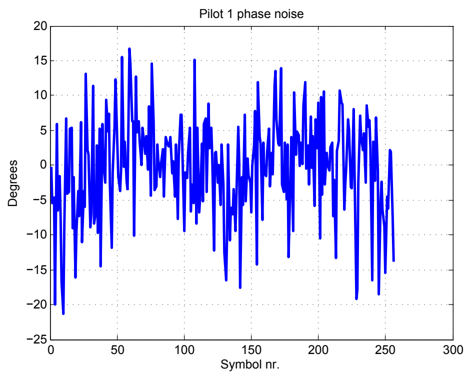

Fig. 10. Phase noise for pilot 1.

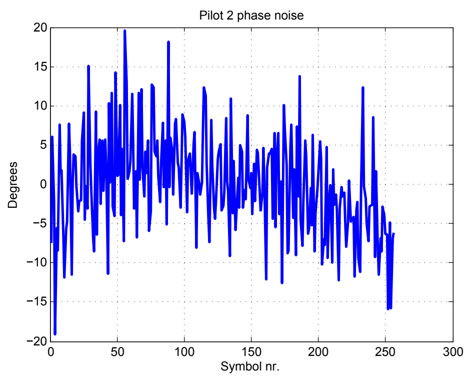

Fig. 11. Phase noise for pilot 2.

The phase noise of the first pilot is given in Figure 10 and for the second pilot in Figure 11. The phase noise is centered around $0°$ with a variation around $\pm 10°$ for both pilot sequences, indicating accurate channel estimates, usable for spatial demultiplexing. The remaining phase shift is also estimated and compensated for. These results are shown in Figures 12 and 13, with a similar spread of both pilots in the scatterplot, due to the phase noise.

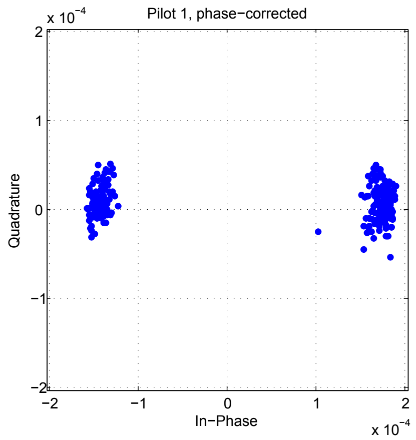

Fig. 12. Corrected scatterplot with phase offset for pilot 1.

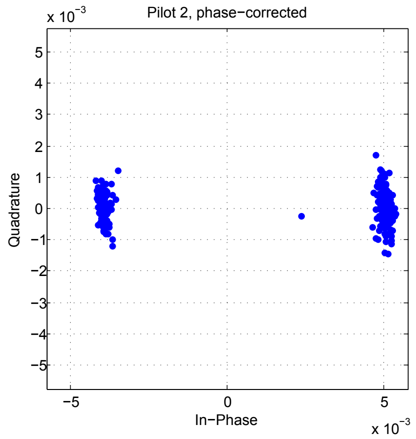

Fig. 13. Corrected scatterplot with phase offset for pilot 1.

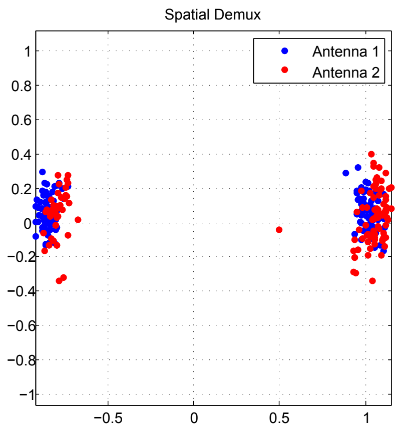

Fig. 14. Spatial demultiplexed signal on both antennas.

The final step is the demultiplexing of the data signal in order to detect the spatially modulated bits, corresponding to the values 1 and -1 for transmit antennas 1 and 2, respectively. This results in Figure 14, showing a symmetric received signal constellation and a correct demodulation of BPSK. Given the dramatic difference in amplitudes for signals originating from different transmit antennas, as indicated by the scale of Figures 12 and 13, the scatterplot in Figure 14 indicates an error free determination of the antenna from which each individual symbol was transmitted. In the latter figure, the received BPSK constellation is plotted with compensation for the channel gains corresponding to each individual symbol, resulting in a normal BPSK constellation, despite the large difference in complex channel gains. The results indicate that it is perfectly possible to capture the correct information bits, even at lower signal-to-noise ratios than present in this particular experiment.

V. Conclusions

A Spatial Modulation Transmitter was successfully designed and practically implemented on a printed-circuit board, transmitting a BPSK signal on a 2.45 GHz RF-carrier and spatially modulating this signal on two antennas. The full design including all key components is documented, as well as the full schematic diagram. The measurement results indicate a correct operation of the system. The transmitted signals are received and demodulated correctly. The data can be correctly detected as well as spatially demultiplexed. Both the bits conveyed in the BPSK symbols as well as the bits encoded in the selected antenna numbers are detected at a very low bit error rate.

Acknowledgment

The authors want to express their gratitude to Electronics Engineering student Joren De Witte for the fruitful cooperation and the interesting work. Without his efforts, the practical implementation would not have been realized.

References

[1] N. Serafimovski, A. Younis, R. Mesleh, P. Chambers, M. Di Renzo, C.-X. Wang, P. M. Grant, M. A. Beach, and H. Haas, *Practical Implementation of Spatial Modulation*, IEEE Transactions on Vehicular Technology, vol. 62, no. 9, pp. 4511-4523, Nov. 2013.

[2] Silicon Laboratories, *C8051F320/1* [Rev. 1.1], Austin, 2003.

[3] Analog Devices Inc., *Dual 10-bit TxDAC+ with 2x Interpolation Filters AD9761* [Rev. C], Norwood, 2003.

[4] Analog Devices Inc., 0.8 *GHz to* 2.5 *GHz Quadrature Modulator AD8346* [Rev. A], Norwood, 2005.

[5] Mini-Circuits, *Frequency Synthesizer DSN-2520A-219+* [Rev. A], New York.

[6] FOXElectronics, *Model: FXO-HC73 SERIES* [Rev. 28/11/2007], Fort Myers, 2008.

[7] Mini-Circuits, *Ultra High IP3 Amplifier Module HXG-242+* [Rev. A], New York.

[8] Mini-Circuits, *High Isolation Switch RSW-2-25P+* [Rev. G], New York.

[9] Eagle PCB design software, http://www.cadsoftusa.com/

[10] Signalion GmbH, *HaLo 430 Hardware In The Loop MIMO Prototyping & Monitoring Platform*, Dresden.

[11] L. Vallozzi, H. Rogier, and C. Hertleer, *Dual Polarized Textile Patch Antenna for Integration Into Protective Garments*, IEEE Antennas and Wireless Prop. Lett., vol. 7, pp. 440-443, 2008.

[12] M. Scarpello, L. Vallozzi, H. Rogier, and D. Vande Ginste, *High-Gain Textile Antenna Array System for Off-Body Communications*, International Journal of Antennas and Propagation, vol. 2012, doi: [10.1155/2012/573438].

[13] M. Oerder and H. Meyr, *Digital Filter and Square Timing Recovery*, IEEE Transactions on Communications, vol. 36, pp. 605-612, 1988.